Electronic Supplementary Material (ESI) for New Journal of Chemistry.

Electric Supporting Information

Europium amphiphilic naphthalene based complex for the enhancement of linearly polarized luminescence in Langmuir-Blodgett films

Koushi Yoshihara, Masamichi Yamanaka, Shuhei Kanno, Soichi Mizushima, Junko Tsuchiyagaito, Kazuki Kondo, Takahiro Kondo, Daichi Iwasawa **,** Hiroaki Komiya, Akira Saso, Shogo Kawaguchi, Kenta Goto, Shuhei Ogata, Hiromi Takahashi, Ayumi Ishii and Miki Hasegawa

Contents

1. Fig. S1 ^{1}H-NMR.
2. Fig. S2 FT-IR spectra.
3. Fig. S3 Thermal analysis (TG) and differential scanning calorimetry (DSC) of Eu(NaphC15)$_3$.
4. Fig. S4 Eu 3d and N 1s XPS bands of the LB films, (a) LB35 and (b) LB40. The binding energies were corrected by the Au 4f band (84.0 eV).
5. Fig. S5 XRD patterns of LB films of NaphC15 including Gd ion (a) depositing at various surface pressure of 30 (Gd-**LB30**), 35 (Gd-**LB35**) and 40 mN/m (Gd-**LB40**). XRD patterns of NaphC15 with stearic acid (1:10) in the LB film at 20 mN/m (b). Temperature dependence of powder XRD of NaphC15 (c) and Eu(NaphC15)$_3$, (d). There is no temperature dependence, meaning the compounds having NaphC15 take quite stable molecular structure and packing.
6. Fig. S6 Electronic absorption spectra of NaphC15 and naphthalene in chloroform and polarized absorption spectrum of the LB film of NaphC15.
7. Fig. S7 Steady luminescence spectra of Eu complexes in LB films.
8. Fig. S8 Luminescence decay profiles of Eu complexes in LB films and EuNaphC15.
9. Fig. S9 Principal of the setting-up to observe optical waveguide spectra (a) and polarized electronic absorption spectra of **LB35** (b). In the table, the D_p and D_s values show the absorbance at 420 nm for bilayers of **LB30** and **LB35**.
10. Fig. S10 Schematic representation of energy transfer and sensitization of ff emission mechanism.

References

1. Fig. S1 ^{1}H-NMR

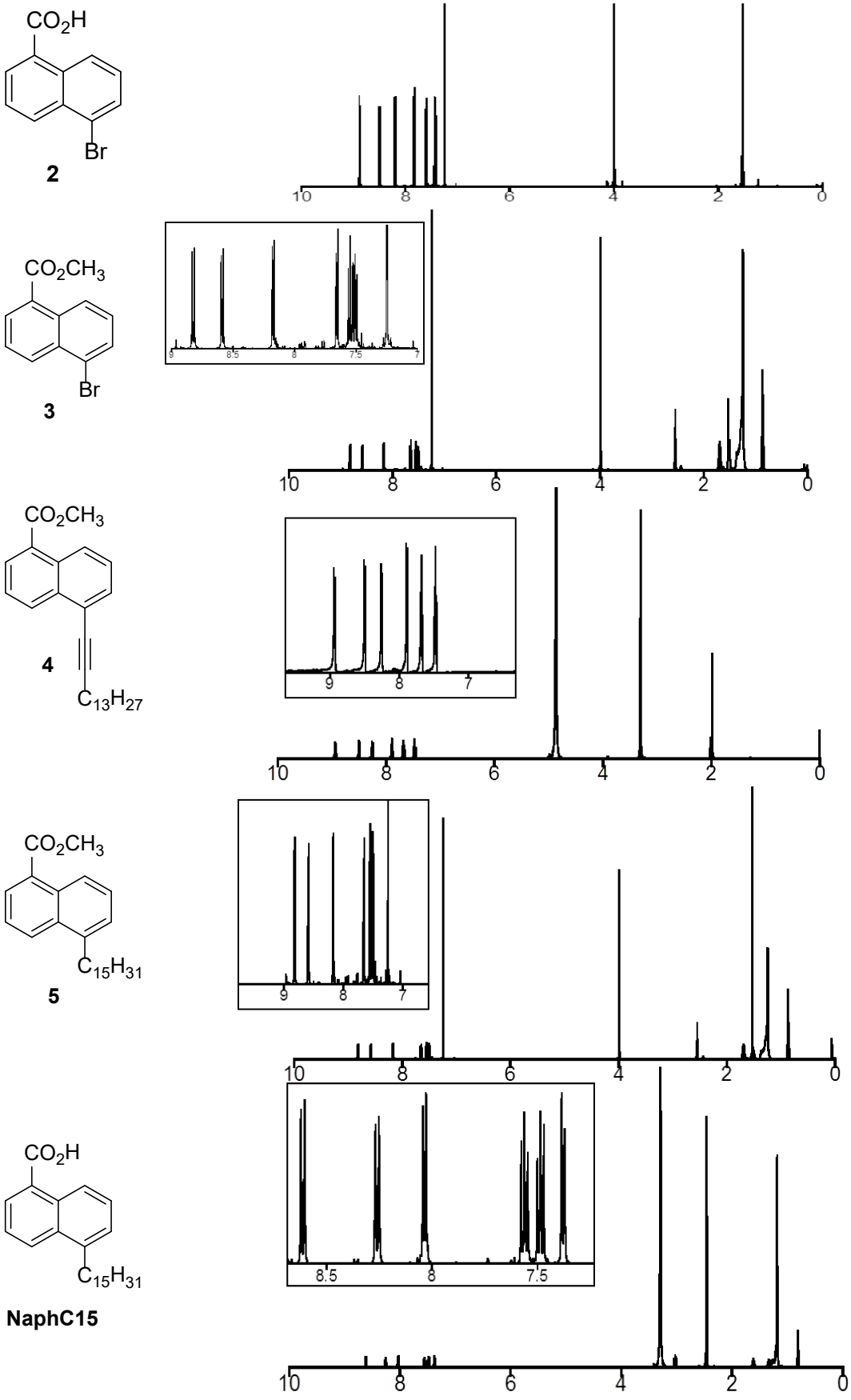

Fig. S1 ^{1}H-NMR of compounds in $CDCl_3$ toward to NaphC15.

2. Fig. S2 ATR FT-IR

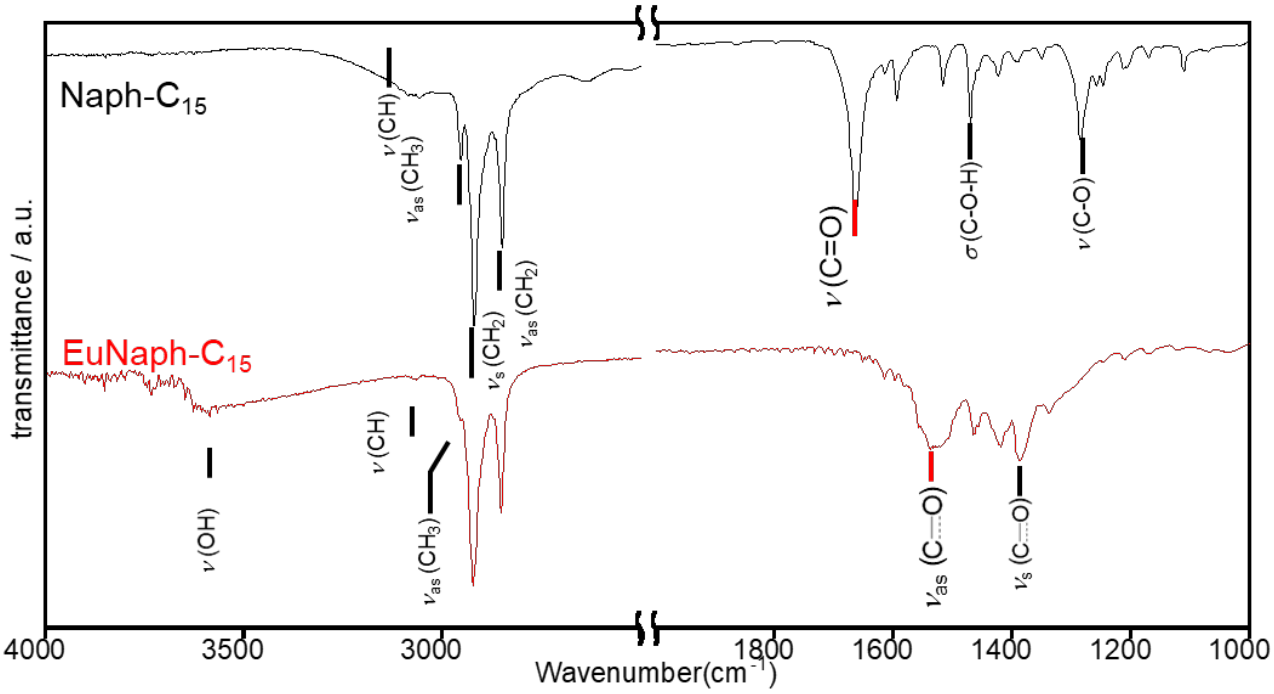

	Wavenumber (cm^{-1})
ν (C-H)	3058
ν (O-H)	3400-3100
$\nu_{as}(CH_2)$	2954
$\nu_{as}(CH_3)$	2917
$\nu_{s}(CH_2)$	2861
$\nu_{s}(CH_3)$	2848
ν (C=O)	1664

Fig. S2 FT-IR spectra of NaphC15 and the Eu complex observed by ATR method without medium.

3. Fig. S3 Thermal analyses

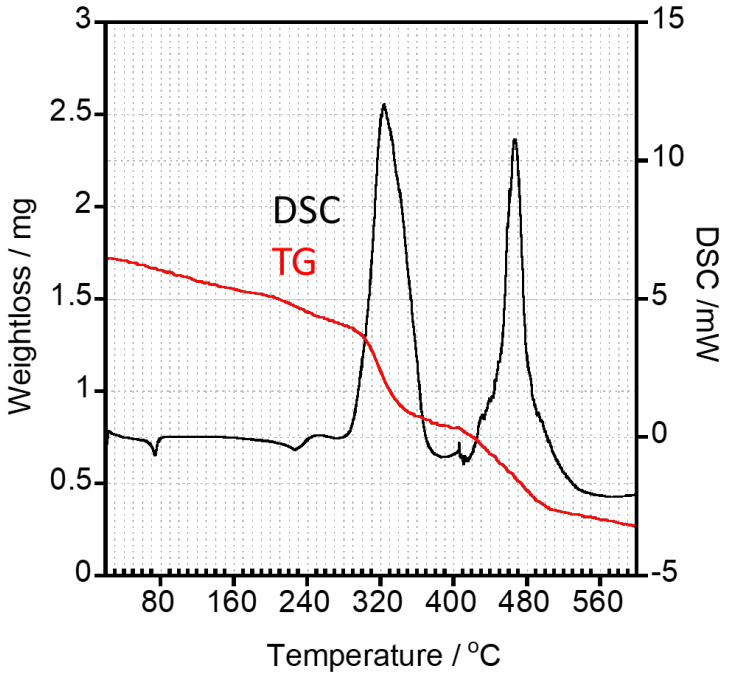

Fig. S3 Thermal gravimetric analysis (TG) and differential scanning calorimetry (DSC) of $Eu(NaphC15)_3$.

4. Fig.S4 XPS bands (Eu 3d and N 1s bands).

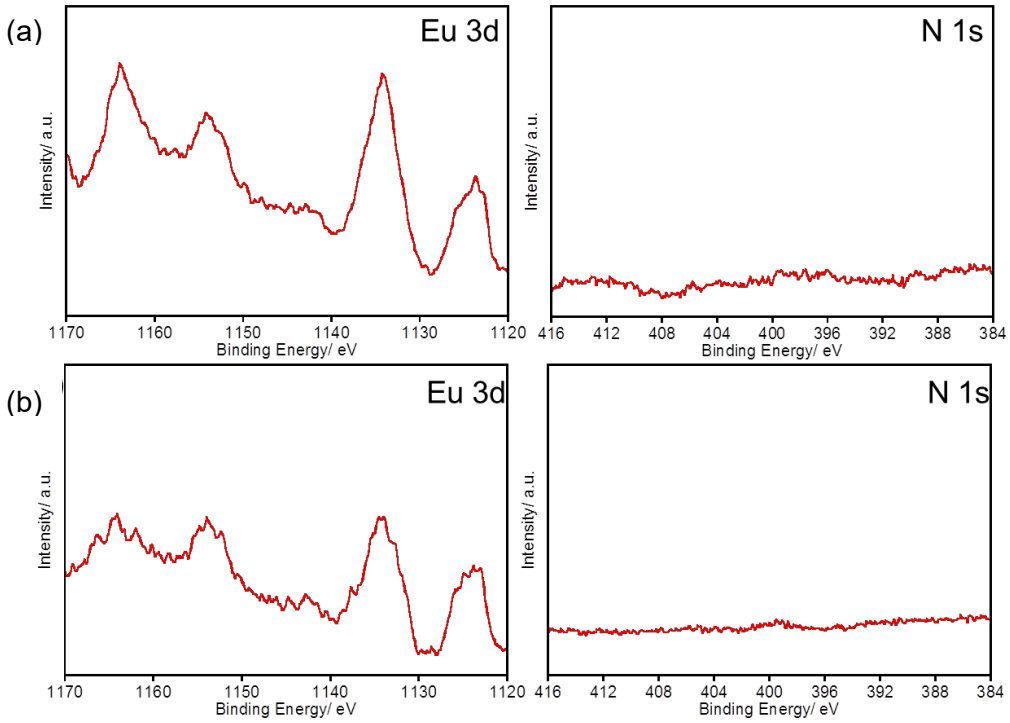

Fig. S4 Eu 3d and N 1s XPS bands of the LB films, (a) **LB35** and (b) **LB40**. The binding energies were corrected by the Au 4f band (84.0 eV).

5. Fig. S5 XRD patterns of the LB films and powders.

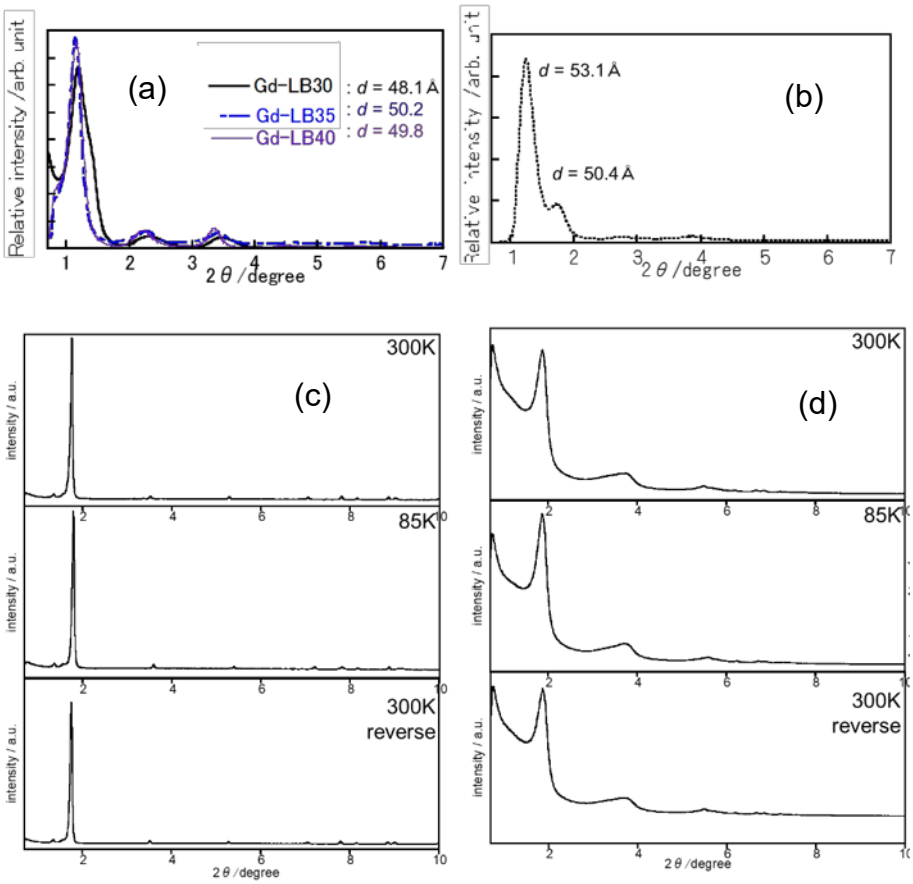

Fig. S5 XRD patterns of LB films of NaphC15 including Gd ion (a) depositing at various surface pressure of 30 (Gd-LB30), 35 (Gd-LB35) and 40 mN/m (Gd-LB40). XRD patterns of NaphC15 with stearic acid (1:10) in the LB film at 20 mN/m (b). Temperature dependence of powder XRD of NaphC15 (c) and $Eu(NaphC15)_3$ (d). There are no temperature dependence, meaning the compounds having NaphC15 take quite stable molecular structure and packing.

6. Fig. S6 Electronic absorption and polarized absorption spectra of NaphC15.

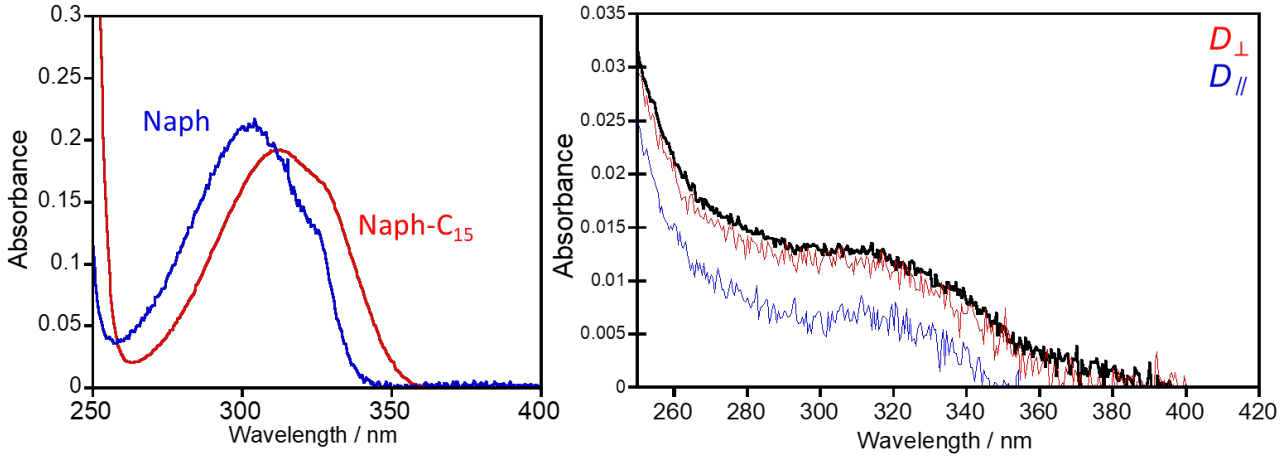

Fig. S6 (left) Electronic absorption spectra of NaphC15 and naphthalene (Naph) in chloroform. The bands of NaphC15 in chloroform appeared at red side compared with those of Naph, since the symmetry of π electronic system in NaphC15 became lower than in Naph. (right) Polarized absorption spectra of the 10 layer-LB film of NaphC15 deposited at 20 mN/m recorded on Shimadzu 3600S with a polarizer attachment. $D_{\perp}$ and $D_{//}$ are optical densities observed with the polarizer angle to perpendicular and parallel, respectively, along the water surface at the LB film formation. Black line is steady absorption spectrum of the film, and the absorbance is normalized at 315 nm.

7. Fig. S7 Steady luminescence spectra of Eu complexes in LB films.

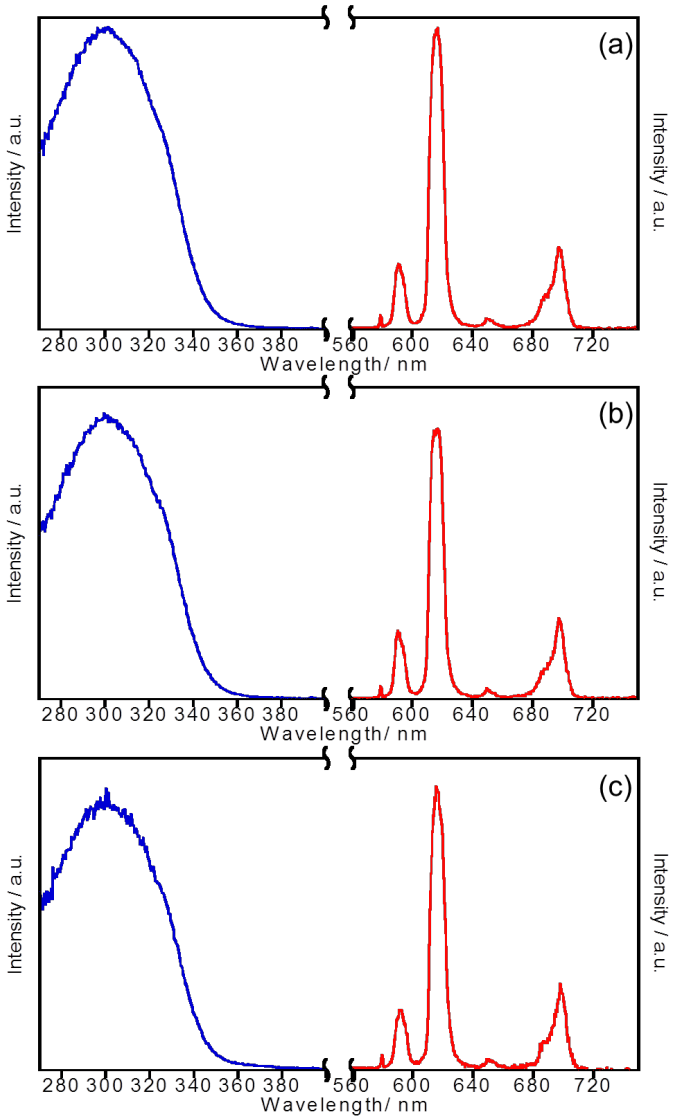

Fig. S7 Steady luminescence (red line; λ_{ex} =310 nm) and excitation (blue line; λ_{mon} =615 nm) spectra of (a) **LB30**, (b) **LB35** and (c) **LB40**.

8. Fig. S8 Luminescence decay profiles of Eu complexes in LB films.

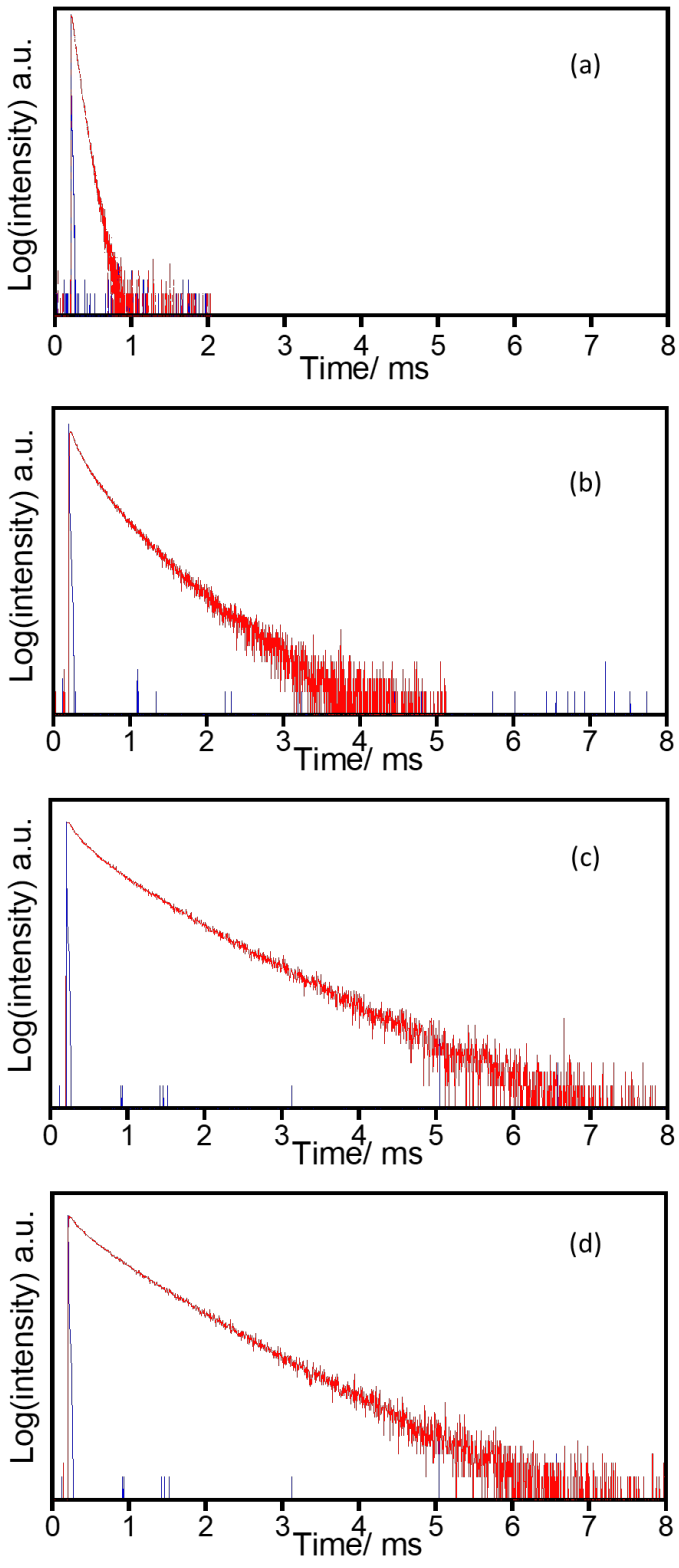

Fig. S8 Luminescence decay profiles of (a) powder of $Eu(NaphC15)_3$, (b) **LB30**, (c) **LB35** and (d) **LB40**.

9. Aspects of the tilt angles of π-electronic systems on the substrate.

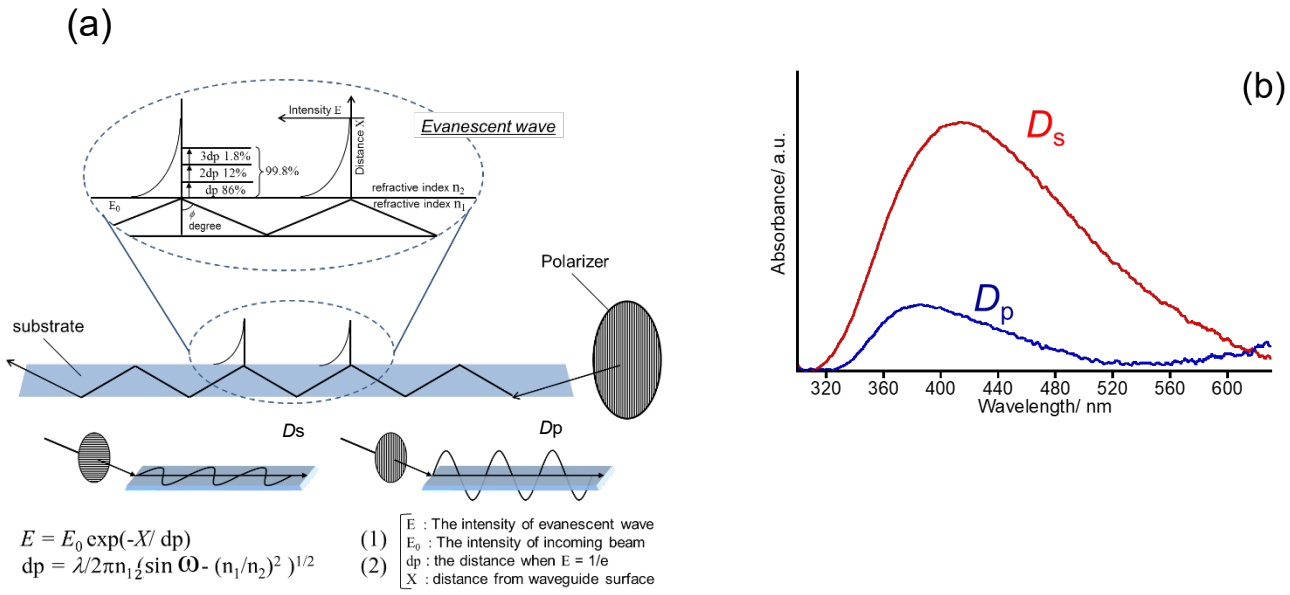

	D_s	D_p
LB30	0.94	0.12
LB35	0.95	0.41

Fig. S9 Principal of the setting-up to observe optical waveguide spectra (a) and polarized electronic absorption spectra of **LB35** (b).[1] In the table, the D_p and D_s values show the absorbance at 420 nm for bilayers of **LB30** and **LB35**.

10. **Fig. S10 Schematic representation of energy transfer and sensitization of ff emission mechanism.**

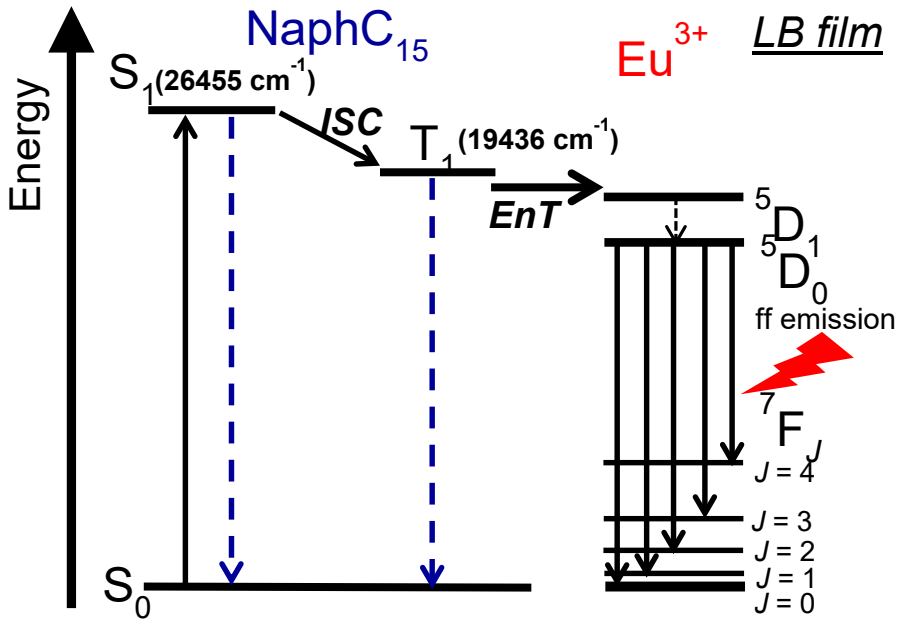

Fig. S10 Schematic representation of energy transfer and sensitization of ff emission Eu in the LB films with NaphC15.

References

[1] D. M. Cropek and P. W. Bohn, *J. Phys. Chem.*, 1990, **94**, 6452-6457.